Journal of Electroanalytical Chemistry 907 (2022) 116035

Contents lists available at ScienceDirect

Journal of Electroanalytical Chemistry

journal homepage: www.elsevier.com/locate/jelechem

Haptenation of skin sensitizers with cysteine and gold nanoparticles modified screen printed carbon electrode analyzed using impedance technique

Teh Ubaidah Noh [b,c], Azila Abdul-Aziz [a,c,*]

[a] Department of Chemical and Environmental Engineering, Malaysia-Japan International Institute of Technology, Universiti Teknologi Malaysia Kuala Lumpur, Jalan Sultan Yahya Petra, 54100 Kuala Lumpur, Malaysia
[b] Bioprocess and Polymer Engineering Department, Faculty of Chemical and Energy Engineering, Universiti Teknologi Malaysia, 81310 Skudai, Johor, Malaysia
[c] Institute of Bioproduct Development, Universiti Teknologi Malaysia, 81310 Skudai, Johor, Malaysia

ARTICLE INFO

Keywords:
Haptenation
Cysteine
Skin sensitizer
Impedance
Charge transfer resistance

ABSTRACT

Skin sensitization is defined as an allergic response to a skin sensitizer upon contact with the skin. Skin sensitization is induced through covalent binding of a skin sensitizer to skin proteins (haptenation process). In this research work, the working electrodes of screen printed carbon electrodes (SPCEs) were modified by electrodepositing gold nanoparticles (AuNPs), addition of thiourea and then followed by self–assembly of AuNPs and cysteine (designated as ETSC). The main purpose of this research was to study the interaction of skin sensitizers with the cysteine and gold nanoparticles modified screen printed carbon electrode (SPCE) analyzed using impedance technique. The interaction of maleic anhydride (as extreme/strong skin sensitizer) with the cysteine modified SPCE was found to result in high changes in the value of charge transfer resistance of skin sensitizer ($\Delta R_{CT}^{skinsensitizer}$) compared to moderate sensitizer (isoeugenol) and weak/non skin sensitizer (glycerol). The ETSC modified SPCE with skin sensitizers were characterised using Fourier–Transform infrared spectroscopy–attenuated total reflectance (FTIR–ATR), atomic force microscopy (AFM) and electrochemical impedance spectroscopy (EIS). The presence of skin sensitizers on the working electrode of ETSC modified electrode was detected by FTIR–ATR. AFM images indicated different patterns with different surface roughness for extreme/strong, moderate and weak/non skin sensitizers. Using EIS, the estimation for fractional surface coverage (θ^{IS}) of ETSC modified SPCE when contacted with maleic anhydride was higher than isoeugenol and glycerol. Other than that, the active site radius (r_a), and the distance between two adjacent sites ($2r_b$) for ETSC modified SPCE when contacted with maleic anhydride were shorter than the r_a and 2rb obtained for isoeugenol and glycerol, indicating higher surface average roughness for ETSC modified SPCE that was contacted with maleic anhydride. Data obtained from EIS agreed with images obtained using AFM. The adsorption kinetic studies for ETSC modified SPCE with skin sensitizers showed that the skin sensitizers displayed Langmuir isotherm adsorption. This work showed that the ETSC modified SPCE has the potential to be employed for the screening of potential skin sensitizers during the early stage of cosmetic and personal care products development.

1. Introduction

Allergic contact dermatitis (ACD) occurs when an active local immune response is stimulated by cutaneous inflammation [1]. Skin sensitization represents an enhancement of immunological reactivity for a specific hapten (skin sensitizer). Kostner et al. [2] reported that the small allergenic molecule (hapten) penetrated the skin and covalently bound to a carrier protein to form a hapten–protein complex. The hapten is a small molecule that must be bound to proteins to be recognised by the immune system. The majorities of occupationally related haptens are reactive, electrophilic chemicals, or metabolised to reactive metabolites that form covalent bonds with nucleophilic centres on the peptide [3]. This characteristic is usually manipulated by researchers for assessing skin sensitizer potential of a substance

* Corresponding author at: Department of Chemical and Environmental Engineering, Malaysia-Japan International Institute of Technology, Universiti Teknologi Malaysia Kuala Lumpur, Jalan Sultan Yahya Petra, 54100 Kuala Lumpur, Malaysia
E-mail address: r-azila@utm.my (A. Abdul-Aziz).

https://doi.org/10.1016/j.jelechem.2022.116035
Received 24 July 2021; Received in revised form 6 January 2022; Accepted 8 January 2022
Available online 12 January 2022

[4]. The –SH group of peptide is a strong nucleophile and has been frequently studied for assessing hapten (skin sensitizer) reactivity [5]. Haptenation occurs from the formation of a stable adduct between haptens and the endogenous peptide in the skin. Any allergen that can make a stable hapten–peptide conjugate is hypothesized to be able to induce skin sensitization [6].

Skin sensitization analysis is one of the required safety assessments of chemicals in products that are applied to the skin [7]. The European Union Reference Laboratory for Alternatives to Animal Testing (EURL ECVAM) committee has validated alternative non–animal testing methods for replacement of the animal testing in skin sensitization studies, namely, direct peptide reactivity assay (DPRA), ARE–Nrf2 Luciferase Test Method (KeratinoSens^{TM}), U937 cell line activation test (U–SENS), Interleukin–8 reporter gene assay (IL–8 Luc assay) and human cell line activation test (h–CLAT) [8]. At least 2 out of 3 negative results are needed to meet regulatory requirements as a single alternative non–animal testing method has not been able to provide enough information due to the complexity of the skin sensitization endpoint in comparison to animal testing methods data [9]. DPRA is an *in chemico* test method that addresses quantitative peptide reactivity that is postulated to be the molecular initiating event of skin sensitization (first key event). Reactivity is measured by analyzing the interaction between the substances or skin sensitizers to the synthetic heptapeptides such as cysteine and lysine. This test method was adopted in 2015 under the standard test method Organisation for Economic Cooperation and Development (OECD) 442C [10].

Over the years, the modifications of DPRA and Amino acid Derivative Reactivity Assay (ADRA) have been studied by the Japanese Centre for the Validation of Alternative Methods (JaCVAM) [11,12,13] followed by an independent peer-review [14]. Even though the DPRA assay identifies skin sensitizers with approximately 80% accuracy [15,16], it still suffers from low detection sensitivity and as such a high concentration of skin sensitizers is required during analysis. This limitation leads to the precipitation of skin sensitizers during the peptide depletion process. To address this issue, Fujifilm has developed the ADRA test method. The ADRA test method allows testing of poorly soluble skin sensitizers. As such, the ADRA test method could complement DPRA data test method.

To enhance the sensitivity of the DPRA assay further, nuclear magnetic resonance spectroscopy (NMR)-based method was proposed by Chittiboyina [17]. The reactivity and classification of potential skin sensitizers were studied using thiol as a nucleophile. NMR spectroscopy was used as the tool for estimating the reactivity of the skin sensitizer reaction. Andres [18] reported another evolution of the DPRA assay using Mass Spectrometry HPLC/MS-MS. A more specific detection of the interaction between peptide to complex mixtures was obtained by incubating reference chemicals and providing quality controls at low, medium, and high concentrations. Wei [19] tried to improve the DPRA assay throughput, accuracy and sensitivity by using an automated 384-well plate-based RapidFire solid-phase extraction (SPE) system coupled with mass spectrometry (SPE-MS/MS-based DPRA). Throughput was improved from 16 min to 10 s per sample, and substrate peptides usage was reduced from 100 mM to 5 mM.

In the meantime, Achilleos [20] tried to fabricate a skin sensitizer biosensor based on the electrophilic reaction between cysteine, lysine, and histidine and skin sensitizer, and the principle of surface plasmon resonance (SPR). The biosensor was studied to improve the response time and complexity of the wet chemistry based assays currently employed for the detection of skin sensitizers. The SPR biosensor was used to calculate the interaction between a ligand (nucleophilic amino acid) and an immobilized analyte (skin sensitizer/allergen) [21] using the direct binding of protein residues. The result was observed directly through the changes in the refractive index at the surface of the biosensor [22]. The interactions observed that weak allergens could quickly dissociate from the ligand, whereas strong and extreme allergens remained bound to the amino acids. However, the disadvantages of the SPR based skin sensitizer biosensor included long response time requiring a high volume of the sample, high regeneration time, and costly detection technique [23].

Due to the limitation of SPR biosensor technology, this work investigated electrochemical impedance spectroscopy (EIS) as a potential technique to study the interaction of skin sensitizers with cysteine. EIS was carried out to measure the changes in charge transfer resistance of skin sensitizer ($\Delta R_{CT}^{sensitizer}$) as a result of different binding rates of affinity of skin sensitizers to cysteine. Disposable screen-printed carbon electrode (SPCE) modified with gold nanoparticles (AuNPs) and cysteine was proposed to be utilized to address the issue of cost and detection time [24].

The benefits of EIS include high sensitivity, label–free strategy, and simplicity as compared to the SPR biosensor [25]. AuNPs have been widely used in the fabrication of nanotechnology based–biosensor [26]. AuNPs play an important role in improving the specificity and sensitivity of electrochemical biosensors [27]. Gold nanoparticles having thiol end can be conjugated with amino acids to give out positive amino groups. In some research works, a cysteine based self-assembled monolayer was used on top of gold nanoparticles surfaces as cysteine has the capability to interact with gold due the formation of a strong cysteine-gold nanoparticles thiolate bond [28].

Skin sensitization can be induced from the haptenation that occurs between the endogeneous peptide in the skin and the skin sensitizer. This work studied the potential of using cysteine and AuNPs modified SPCE analysed using impedance technique for rapid skin sensitization analysis. In addition, Fourier–Transform infrared spectroscopy–attenuated total reflectance (FTIR–ATR) analysis, Atomic Force Microscopy (AFM) analysis and adsorption kinetics studies were conducted to study the interaction between the skin sensitizers and cysteine.

2. Materials and methods

2.1. Chemicals reagents

Potassium ferricyanide ($K_3Fe(CN)_6$), gold chloride ($HAuCl_4$), trisodium citrate dehydrate ($Na_3C_6H_5O_7$), potassium chloride (KCl) and cysteine ($C_3H_7NO_2S$), which were used for the modification for SPCE, were obtained from Sigma-Aldrich, Malaysia. Maleic anhydride ($C_4H_2O_3$), isoeugenol ($C_{10}H_{12}O_2$) and glycerol ($HOCH_2CH(OH)CH_2$-OH), which were used as models of skin sensitizers, were also purchased from Sigma-Aldrich Chemical Company (Malaysia). All chemicals used were of analytical reagent grade and they were used as received unless otherwise noted.

2.2. Modification of SPCE with electrodeposited AuNPs, Self-assembled AuNPs and cysteine (designated as ETSC)

Disposable SPCEs (10 mm width × 33 mm length × 0.5 mm height) were purchased from Metrohm Malaysia Sdn Bhd. The SPCE consisted of three electrodes: a carbon auxiliary electrode, a carbon working electrode, and a silver/silver chloride reference electrode. AuNP was electrodeposited onto the working electrode by immersing the SPCE in 100 μl of AuNPs and $Na_3C_6H_5O_7$ solutions at a current of + 1.1 V for 60 s using chronoamperometry (Autolab PGSTAT 30 (Switzerland)) based on the method of Mocanua et al. [28] with slight modification. Then, the modified working electrode of the SPCE was deposited with 6 μl of 0.25 mM thiourea to act as a cross-linker between AuNPs monolayers. Next, 6 μl of a solution made up of 0.001 M $HAuCl_4$, 0.1 M cysteine, and 0.5 M H_2SO_4 [29] was dropped onto the surface of the modified working electrode in a petri dish. Lastly, 6 μl of 50 mM cysteine was dropped onto the modified working electrode. The SPCE was then wrapped using parafilm to minimise oxygen exposure.

Table 1
The values of $\Delta R_{CT}^{skinsensitizer}$ upon exposure of ETSC modified SPCE with skin sensitizers of different potency.

Test chemical (Skin sensitizer)	LLNA* EC3 (%)	$\Delta R_{CT}^{sensitizer}$ (Ω)	Category of skin sensitizing potency
Maleic anhydride	0.16	28071.33 ± 1418.84	Extreme/strong
Isoeugenol	1.30	9704.00 ± 40.31	Moderate
Glycerol	NS**	1577.67 ± 161.93	Weak/Non

* LLNA – local lymph node assay (The LLNA EC3 data was referred to as the gold standard for skin sensitization analysis in this work).
** NS– Non sensitizing

2.3. Analysis of the haptenation of skin sensitizers with the modified SPCE

The investigation of the haptenation mechanism for ETSC modified SPCE exposed with maleic anhydride (extreme/strong skin sensitizer), isoeugenol (moderate skin sensitizer), and glycerol (weak/non skin sensitizer) was conducted using Fourier–transform infrared spectroscopy–attenuated total reflectance (FTIR–ATR) analysis to detect the presence of skin sensitizers on working electrode of ETSC modified SPCE. After deposition with skin sensitizers, the ETSC modified SPCEs were analysed using FTIR–ATR (Frontier PerkinElmer: Santa Clara, USA) with energy scanning from 650 to 4000 cm^{-1} [30].

Atomic Force Microscopy (AFM) (JPK BioAFM, Germany) was used to measure the roughness of the ETSC modified SPCE with skin sensitizers surface at a high resolution. The investigation of the haptenation mechanism for ETSC modified SPCEs with maleic anhydride (extreme/strong skin sensitizer), isoeugenol (moderate skin sensitizer), and glycerol (weak/non skin sensitizer) was conducted using AFM to investigate if there were any differences of the surfaces of the AuNPs–cysteine modified SPCEs after interaction with different classes of skin sensitizers. The AFM imaging was done on flat AuNPs–cysteine modified SPCE surfaces evaporated onto silicon substrates.

2.4. Electrochemical impedance spectroscopy (EIS)

EIS is an effective tool to measure the interaction between ETSC modified SPCE modified SPCE with skin sensitizers by interpreting the ΔR_{ct} data [31–33]. The frequency range used in this experiment started from 15,000 Hz to 0.01 MHz with 5 mV amplitude and + 1.0 V potential using Autolab PGSTAT 30 (Switzerland) with frequency response analysis (FRA) software version 4.9. 6 μl (~ca.) of one millimolar skin sensitizer was deposited for a few minutes onto the ETSC modified SPCE [31]. Then, the ETSC modified SPCEs was immersed in 1 mM of $K_3Fe(CN)_6$ in 0.1 M KCl.

Surface areas of the ETSC modified SPCE with skin sensitizer were estimated by comparing the fractional surface coverage (θ^{IS}), active site radius (r_a), and the distance between two adjacent sites ($2r_b$) values. Matsuda et al. [34] and Finklea et al. [35] have derived equations for the impedance of electrodes having θ^{IS} values lower and greater than 0.9, assuming equal concentrations and diffusion coefficients of the oxidized and reduced species. According to Finklea et al. [35], the equations for the real Faradaic impedance are similar for both situations, except for the value of the parameter q, which describes the relationship between the diffusion coefficient and the microelectrode dimensions. For $(1 - \theta^{IS})$ greater than 0.1 and $(1 - \theta^{IS}) < 0.1$, Eq. (1), (2) and (3) that describe the real Faradaic impedance are given as:

$$Z_f' = \frac{R_{CT}}{1-\theta^{IS}} + \frac{\sigma}{\sqrt{\omega}} + \frac{\sigma}{1-\theta^{IS}}\left\{\frac{\left[(\omega^2+q^2)^{\frac{1}{2}}+q\right]}{(\omega^2+q^2)}\right\}^{\frac{1}{2}} \quad (1)$$

where, R_{CT}, σ, and ω, and q can be obtained from Eq. (5) or (6) [31]

$$q = \frac{2D}{[r_b^2\theta^{IS}(1-\theta^{IS})\ln(1+\frac{0.27}{1-\theta^{IS}})^{\frac{1}{2}}]} \text{for}(1-\theta^{IS}) > 0.1 \quad (2)$$

$$q = \frac{D}{0.36r_a^2} \text{for}(1-\theta^{IS}) < 0.1 \quad (3)$$

The Faradaic impedance for high frequencies is described by Eq. (4) [4]:

$$Z_f' = \frac{R_{CT}}{1-\theta^{IS}} + m\omega^{-\frac{1}{2}} \quad (4)$$

where,

$$m = \sigma + \frac{\sigma}{1-\theta^{IS}} \quad (5)$$

$$(1-\theta^{IS}) = \frac{ra^2}{rb^2} \quad (6)$$

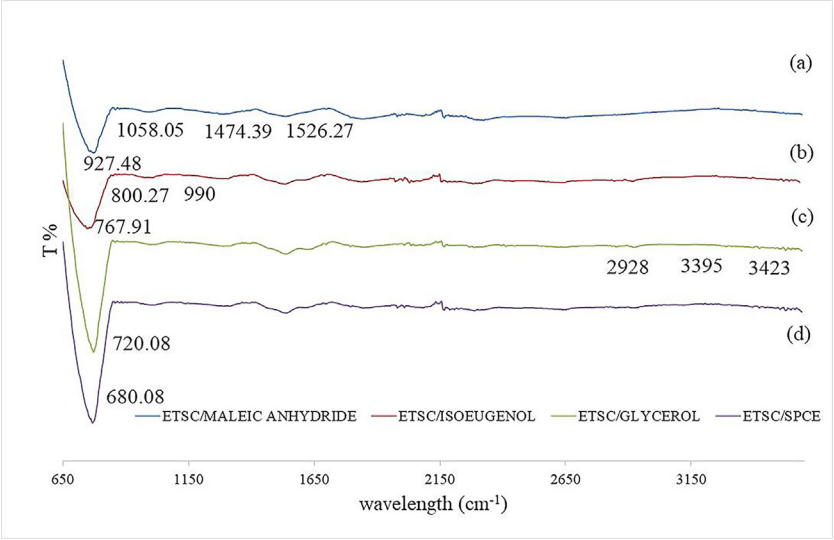

Fig. 1. The FTIR-ATR graph of (a) maleic anhydride, (b) isoeugenol and (c) glycerol with (d) ETSC modified SPCE.

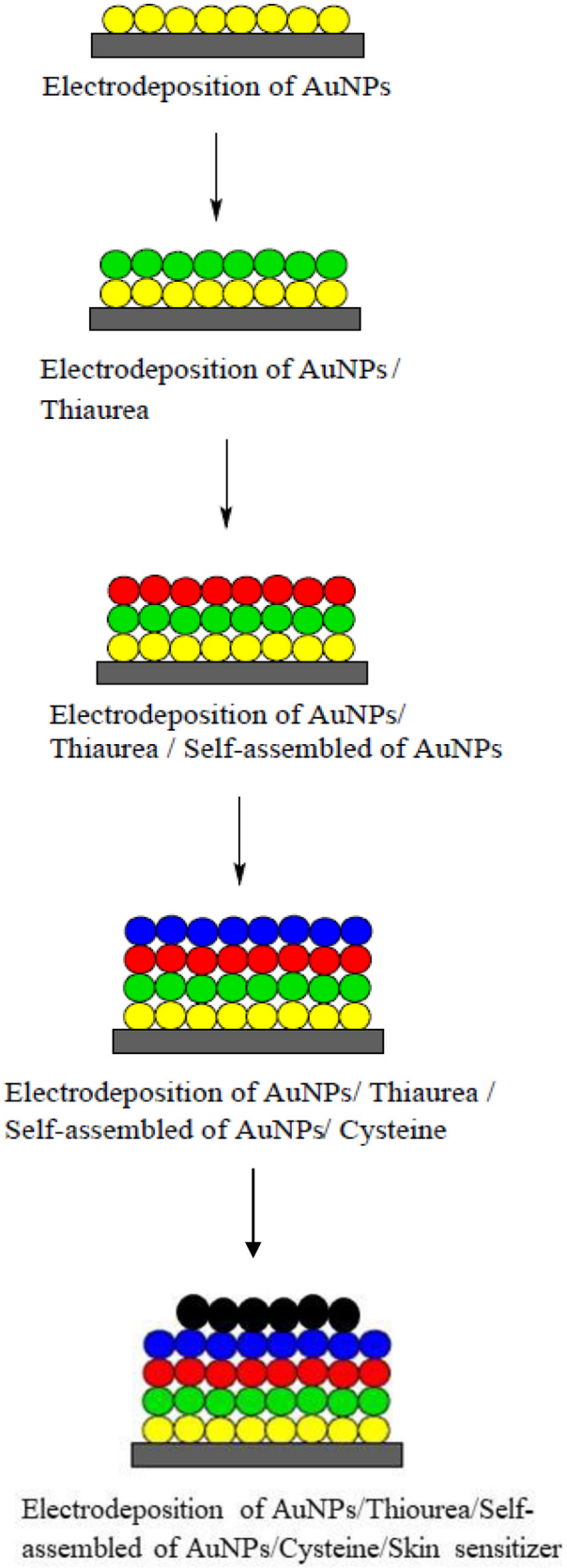

Fig. 2. Illustration of ETSC modified SPCE with skin sensitizer.

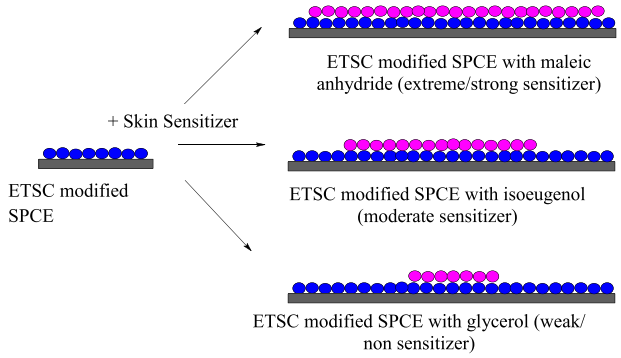

Fig. 3. The schematic model of ETSC modified SPCE immobilized with potential skin sensitizers (maleic anhydride, isoeugenol, and glycerol).

2.5. Adsorption kinetics studies of skin sensitizers for ETSC modified SPCE

6 μl of skin sensitizers (maleic anhydrides, isoeugenol, and glycerol) solution having concentrations ranging from 0.001 M to 0.01 mM was dropped onto the surface of ETSC modified SPCEs [31]. After a few minutes, the ETSC modified SPCEs that was immobilised with the skin sensitizer was washed with distilled water and left to dry under flowing air. Then the ETSC modified SPCEs were immersed in 1 mM of $K_3Fe(CN)_6$ in 0.1 M KCl solution and EIS measurements were taken.

The values of the degree of surface coverage (θ_{SC}) of the skin sensitizers were obtained from $\Delta R_{CT}^{skinsensitizer}$ measurements. θ_{SC} values were calculated based on the ratio of $\Delta R_{CT}^{skinsensitizer}/\Delta R_{CT}^{ETSCmodifiedSPCE}$. To gain information on the adsorption kinetics of the skin sensitizers on the cysteine modified SPCE surface, a plot of C_i/θ_{SC} against C_i was obtained based on Equation (7) [37,38]:

$$C_i/\theta_{SC} = 1/K_b + C_i \quad (7)$$

where C_i is the concentration of skin sensitizer, and K_b represents the binding rate constant of the skin sensitizer on the cysteine modified SPCE surface.

3. Results and discussion

3.1. The effect of different classes of skin sensitizers on R_{CT}

EIS was used to measure the potential interaction between known skin sensitizers of different classes (maleic anhydride, isoeugenol and glycerol) with the modified SPCE. Maleic anhydride is a strong skin sensitizer and isoeugenol is a moderate skin sensitizer. Glycerol, however, is categorized as a weak/non skin sensitizer. This study aimed to investigate whether $\Delta R_{CT}^{skinsensitizer}$ values from impedance data of the potential interaction between the skin sensitizers and the ETSC modified SPCE would significantly be quantified and the differences of the values be recorded based on the substance's sensitization potency. The results, as summarized in Table 1, demonstrate that an association between the $\Delta R_{CT}^{skinsensitizer}$ reactivity and sensitization potency was evident. The interaction between ETSC modified SPCE with maleic anhydride resulted in the highest value of $\Delta R_{CT}^{skinsensitizer}$ compared to the interaction between ETSC modified SPCE with glycerol. $\Delta R_{CT}^{skinsensitizer}$ was calculated using Eq. (10).

$$\Delta R_{CT}^{skinsensitizer} = R_{CT}^{ETSCmodifiedSPCEwithskinsensitizer} - R_{CT}^{ETSCmodifiedSPCEwithoutskinsensitizer} \quad (10)$$

It is believed that the formation of a hapten–protein complex is a prerequisite for the initiation of skin sensitization. Thus, an electrophilic skin sensitizer (hapten) is believed to react with the nucle-

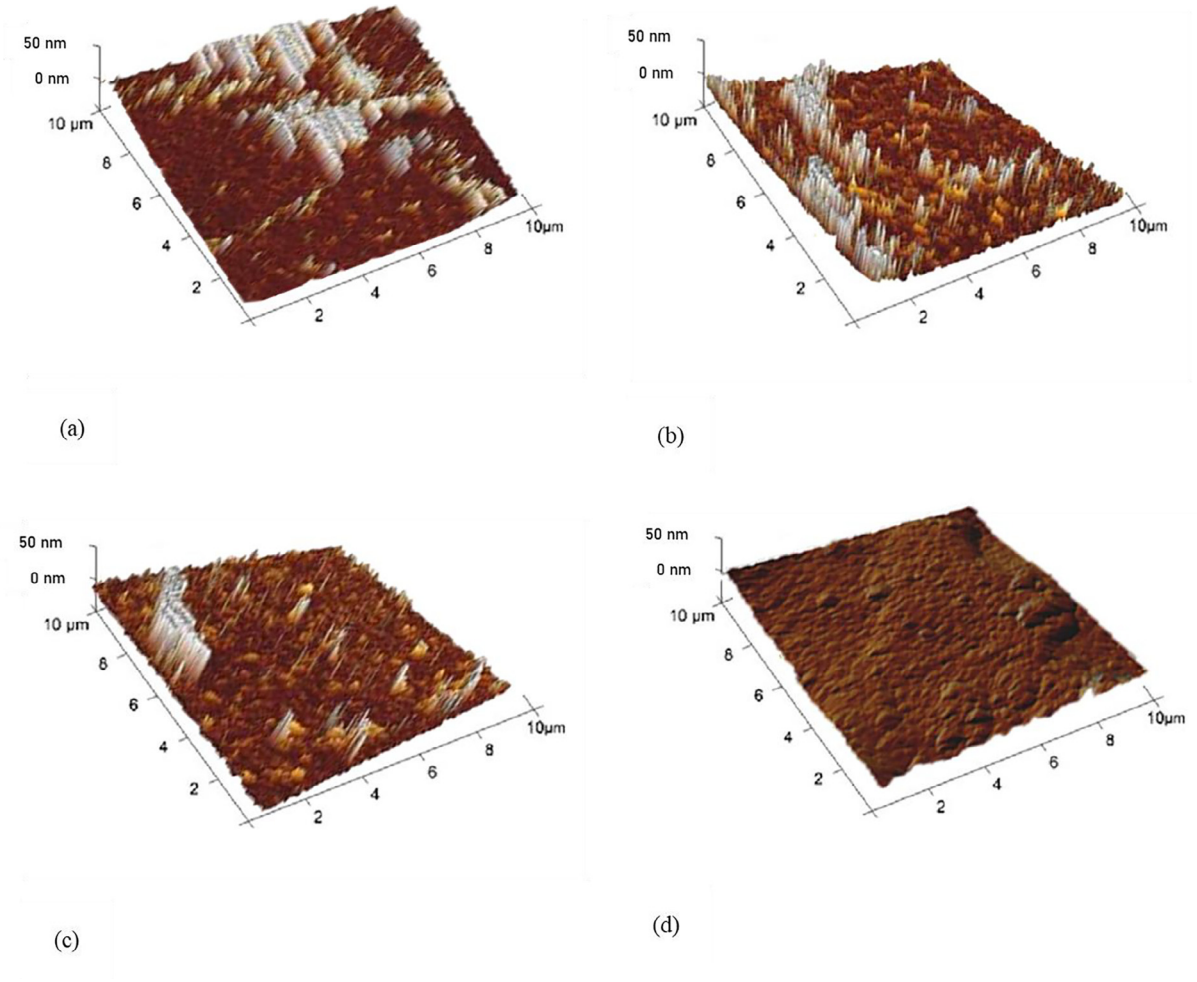

Fig. 4. AFM images of (a) maleic anhydride, (b) isoeugenol, and c) glycerol with (d) ETSC modified SPCE.

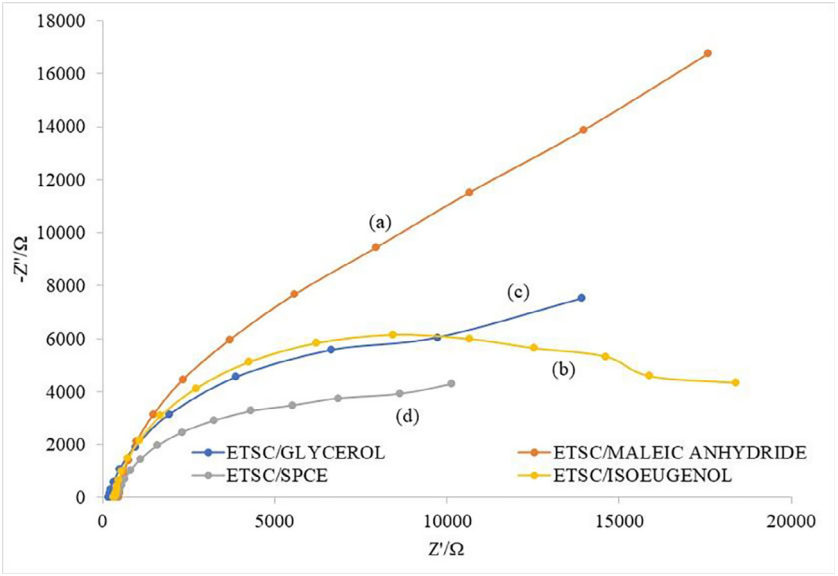

Fig. 5. The Nyquist plots of − Z' and − Z″ for (a) maleic anhydride, (b) isoeugenol and (c) glycerol with (d) ETSC modified SPCE with. Working electrode area = 0.1256 $cm^{2.}$

ophilic amino acids (in this work: cysteine) to form a stable covalent bond which is critical to the initiation of a skin sensitization response. Protein thiol reactivity appears to be a good indicator of skin sensitization hazard. The reaction of chemicals with protein thiol leads to the

Table 2
Parameters used to fit the ETSC modified SPCE with maleic anhydride, isoeugenol, and glycerol for impedance data.

Modified SPCE+ skin sensitizer	Rs (Ωcm^2)	CPE1 ($\mu S\ cm^2 S^{\alpha-1}$)	α_1	$R_{CT.app}$ (Ωcm^2)	CPE2 ($\mu S\ cm^2 S^{\alpha-1}$)	α_2	R (Ωcm^2)	s^2
ETSC + maleic anhydride	22.39	1.44	0.92	4097.83	11.09	0.40	773.34	6.13×10^{-3}
ETSC + isoeugenol	24.34	16.83	0.94	3290.59	13.07	0.39	4.840	5.03×10^{-2}
ETSC + glycerol	22.40	4.17	0.91	1494.64	8.98	0.78	1169.14	4.30×10^{-4}

$R_{CT.app}{}^{a} = \frac{R_{CT}}{(1-\theta)}$; capacitance = CPE $(\omega_{max})^{\alpha-1}$.

formation of bonds of different strengths. Table 1 suggests the possibility of quantifying the interaction between the known skin sensitizers of different strengths and the ETSC modified SPCE. This provides an interesting avenue of the possibility of rapid detection of skin sensitization potential of a chemical. However, the significance of the differences in the values obtained need to be probed further.

3.2. FTIR-ATR spectroscopy analysis of the interaction between ETSC modified SPCE with skin sensitizers

Fig. 1 shows FTIR–ATR spectra of the interaction of maleic anhydride, isoeugenol and glycerol with ETSC modified SPCE. The recorded peaks in Fig. 1(a) belong to characteristics anhydrides group (C═O bond at 1474.39 and 1526.27 cm^{-1}, C—O bond at 1058.05, and at 927.48 cm^{-1}) [39]. The presence of these peaks suggested the immobilisation of maleic anhydride on the ETSC modified SPCE's surface [31]. For isoeugenol, the peaks obtained belong to aromatic compound groups (around 767.91 cm^{-1}), amide (stretch of C—H bond at 800.27 cm^{-1}) and alkene (possible stretch of 990 cm^{-1}) [39] (Fig. 1 (b)). The presence of these peaks suggested the immobilisation of isoeugenol on the ETSC modified SPCE's surface [40,41]. In Fig. 1(c), the characteristic alcohol group (O—H bond) of glycerol was recorded at a peak around 3395 and 3423 cm^{-1}, and a stretch of C—H bond was recorded at around 2928 cm^{-1}. The results are in agreement with the previous work carried out by Basketter et al [42,43]. Also, the presence of a possible stretch of C—S bond at around 680.08 cm^{-1} and 720.08 cm^{-1} (Fig. 1) suggested the immobilisation of cysteine on the ETSC modified SPCE's surface. These analyses suggested the presence of maleic anhydride, isoeugenol, and glycerol after the skin sensitizers interacted with the ETSC modified SPCE.

3.3. AFM images of the ETSC modified SPCE after interaction with skin sensitizers

Figs. 2 and 3 illustrate the schematic model of the layers of ETSC modified SPCE and the possible interaction between the ETSC modified SPCE and the skin sensitizers, respectively. AFM analysis was performed to analyse the surface roughness of the ETSC modified SPCEs after haptenation with skin sensitizers (Fig. 4). Average surface roughness was expected to vary based on the affinity of cysteine towards the skin sensitizers. AFM images exhibit a variety of structures, including linear arrangement, distortion and randomly packed structure due to particles interactions [44,45]. The height of peak can be measured and was used to characterise the dimension of the interactions of the ETSC modified SPCE with maleic anhydride, isoeugenol, and glycerol.

Fig. 4(a), shows the 3D image profile of ETSC modified SPCE which was bound with maleic anhydride. The maleic anhydride bound on ETSC modified SPCE surfaces had a very high average roughness (R_a) of ± 35.59 nm with an average height of ± 50 nm. Maleic anhydride on ETSC modified SPCE resulted in rough planar surface with low peak spacing and spike indicating a thick layer topping.

The adsorption of maleic anhydride onto the ETSC modified SPCE surface was postulated to be due to bonding between the alkoxy group of maleic anhydride and − SH functional groups. The bond formation was due to electrostatic interaction from the nucleophilic addition and the binding mechanism of maleic anhydride with cysteine was suggested to be through strong covalent bonding by Michael acceptors mechanism [5].

The 3D image profile of isoeugenol on ETSC modified SPCE was different from that of ETSC modified SPCE exposed with maleic anhydride surface as shown in Fig. 4(b). Isoeugenol on ETSC modified SPCE surface electrode was dense and homogeneous with many globular aggregates. The interaction of covalent binding for isoeugenol and sulfur was hypothesized to be due to pro–Michael acceptors mechanism. The reaction resulted in nucleophilic addition on the benzene group of isoeugenol [5]. Within the SAM, isoeugenol molecules were densely packed on the surface of ETSC modified SPCE with normal molecular orientation, where their electrophilic groups were firmly attached to

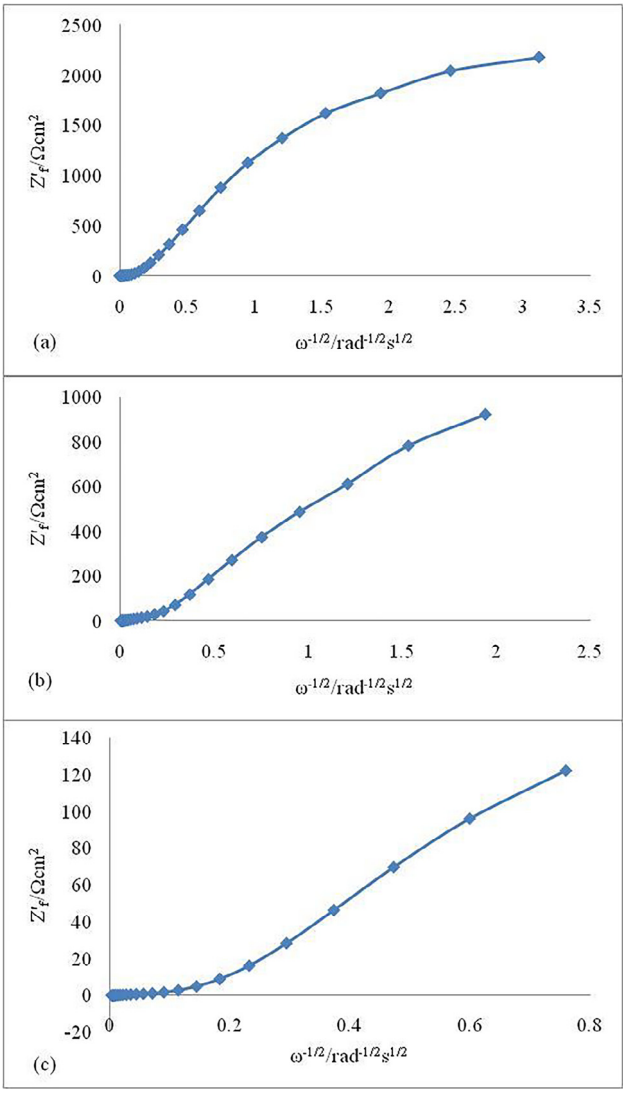

Fig. 6. The Faradaic impedance plots of Z'_f and $\omega^{-1/2}$ for ETSC modified SPCE with (a) maleic anhydride, (b) isoeugenol, and (c) glycerol.

Table 3
The value of θ^{p}_{IS}, r_a, and 2 r_b for ETSC modified SPCE with different skin sensitizers.

Type of modified SPCE	θ^{p}_{IS}	Slope, m ($\Omega cm^2\ rad^{1/2}s^{-1/2}$)	r_a (μm)	2 r_b (μm)
ETSC + maleic anhydride	0.9800	1274.52	2.50	15.99
ETSC + isoeugenol	0.9536	563.66	4.73	21.96
ETSC + glycerol	0.8757	226.23	7.08	40.20

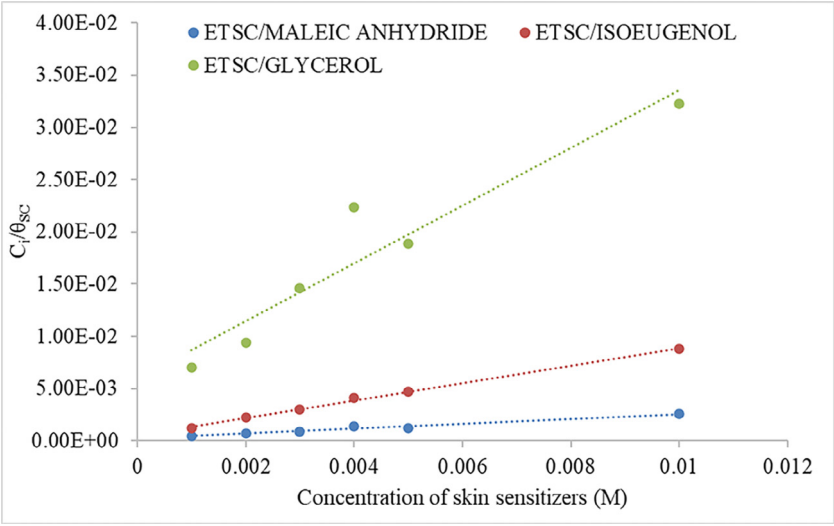

Fig. 7. Plots of C_i/θ_{SC} against concentrations of (a) maleic anhydride, (b) isoeugenol, and (c) glycerol on ETSC modified SPCE in 0.1 M KCl containing 1 mM of $Fe(CN)_6^{3-/4-}$ at 10 mV/s.

the electrode surface with thiols functional groups serving as surface groups. This arrangement resulted in R_a of ± 16.74 nm with an average height of ± 30 nm.

Fig. 4(c) shows the 3D image profile of glycerol immobilized onto the surface of the ETSC modified SPCE monolayer. Compared to isoeugenol molecules on ETSC modified SPCE in Fig. 4(b), glycerol molecules on ETSC modified SPCE was aggregated to smoother globes (average height of ± 15 nm) and were not as compact as isoeugenol molecules on ETSC modified SPCE monolayers. The SAM of glycerol resulted in the lowest R_a at ± 10.62 nm on the ETSC modified SPCE surface.

All the AFM images show that attachment of maleic anhydride, isoeugenol, and glycerol onto the ETSC modified SPCE surface were observed, and the patterns varied according to the class of the skin sensitizer. The AFM analysis correlated with the $\Delta R_{CT}^{skinsensitizer}$ data. The increase in the $\Delta R_{CT}^{skinsensitizer}$ data was postulated to be due to the surface roughness and height of the immobilisation surface after attachment with the skin sensitizers. In this work, AFM had been shown to be a suitable method for analyzing the haptenation process of ETSC modified SPCE with skin sensitizers. The observed trend for the ETSC modified SPCE with skin sensitizers was in good agreement with the trend observed for average surface roughness and height carried out in similar work by [44] and [28].

3.4. Estimation of the electrode fractional surface coverage (θ^{IS}), active site radius (r_a), and the distance between two adjacent sites ($2r_b$)

Estimations of the θ^{IS}, r_a, and 2 r_b were obtained by assuming the charge transfer occurred at the active sites and that there were planar diffusions of redox species to these sites [31]. The equivalent circuit (R(Q[R(QR)])) was closely fitted to the experimental impedance data for ETSC modified SPCE with maleic anhydride, isoeugenol, and glycerol, but the mass transfer impedance was not a true Warburg impedance. The results of the fitting of the experimental data are given in Table 2 based on the equivalent circuit. The semicircle diameters located at high frequencies corresponded to the charge transfer reaction followed by a linear region of the (–Z“) vs. (Z') plot at low frequencies. In this frequency region, the impedance response is dominated by the mass transfer of the redox species to and from the electrode surface.

Fig. 5 shows Nyquist plots of ETSC modified SPCE exposed with maleic anhydride, isoeugenol, and glycerol in 0.1 M KCl containing 1 mM of $Fe(CN)_6^{3-/4-}$ at 10 mV/s. As can be seen in Fig. 5, Nyquist plots obtained from ETSC modified SPCE with maleic anhydride, isoeugenol, and glycerol showed large differences between the extreme/strong, moderate, and weak/non skin sensitizer in terms of R_{CT} values (from semicircles diameters) in Table 2.

For the ETSC modified SPCE with maleic anhydride, a value of m = 1274.52 $\Omega \cdot cm^2 \cdot rad^{1/2} \cdot s^{-1/2}$ was obtained from the slope of the Z'_f vs. $\omega^{-1/2}$ plot in the high frequency region (Fig. 6 (a)). The frac-

Table 4
Adsorption kinetic studies for ETSC modified SPCE with skin sensitizer based on the different potency of skin sensitizers.

Type of modified SPCE	ΔG° (kJ/mol)	Dissociation constant, K_d (M)	Binding rate constant, K_b (M^{-1})
ETSC + maleic anhydride	$-2.14 \times 10^{+04}$	0.0002	$5.00 \times 10^{+03}$
ETSC + isoeugenol	$-1.88 \times 10^{+04}$	0.0005	$2.00 \times 10^{+03}$
ETSC + glycerol	$-1.29 \times 10^{+04}$	0.0059	$1.67 \times 10^{+02}$

tional surface coverage for ETSC modified SPCE exposed with maleic anhydride ($\theta^{IS}_{ETSC+MA}$) was found to be 0.98. The estimation of θ^{IS} of ETSC modified SPCE after exposure with maleic anhydride showed a high value (Eq. (1)–(6)). The intersection between high and low frequency domains resulted in a value of q = 5400. The high value of $\theta^{IS}_{ETSC+MA}$ corresponded to the high surface area of ETSC modified SPCE with maleic anhydride and the high affinity of cysteine towards extreme/strong skin sensitizer. Similar findings have been observed in the investigation carried out by Achilleos et al [20]. A possible explanation for such occurrence could be due to the presence of a positive charge on the electrode surface, as discussed earlier.

For the ETSC modified SPCE with isoeugenol, a value of m = 563.66 $\Omega{\cdot}cm^2{\cdot}rad^{1/2}{\cdot}s^{-1/2}$ was obtained from the slope of the Z'_f vs. $\omega^{-1/2}$ plot in the high frequency region (Fig. 6 (b)). From Fig. 6 (b), the fractional surface coverage for ETSC modified SPCE exposed with isoeugenol ($\theta^{IS}_{ETSC+ISO}$) was calculated to be 0.9536. The intersection between high and low–frequency domains resulted in a value of q = 1500. $\theta^{IS}_{ETSC+ISO}$ belongs to moderate skin sensitizer potency, therefore the lower coverage of the surface area of ETSC modified SPCE with isoeugenol compared to maleic anhydride was due to lower stability and weaker interaction between cysteine and isoeugenol. This supported the optimum conditions suggested by Divkovic et al [43,44].

For the ETSC modified SPCE with glycerol, a value of m = 226.23 $\Omega{\cdot}cm^2{\cdot}rad^{1/2}{\cdot}s^{-1/2}$ was obtained from the slope of the Z'_f vs. $\omega^{-1/2}$ plot in the high frequency region (Fig. 6 (c)). From Fig. 6 (c) the fractional surface coverage for ETSC modified SPCE exposed with glycerol ($\theta^{IS}_{ETSC+GLY}$) was determined to be 0.8757. The intersection between high and low–frequency domains resulted in a value of q = 430. The low value of $\theta^{IS}_{ETSC+GLY}$ might be due to low affinity binding of cysteine with glycerol due to no covalent bonding formed during the haptenation process. The trend was also in general agreement with Aptula et al [5].

For the ETSC modified SPCE with maleic anhydride, the estimated r_a and 2 r_b were 2.5 μm and 15.99 μm, respectively (Table 3). The low r_a and 2 r_b values (pinholes/defects size) for ETSC modified SPCE with maleic anhydride suggested an increase in the average surface of roughness and the results agree with the images obtained from AFM. This might be due to the high stability of maleic anhydride molecules immobilised to cysteine producing a significant high binding response. AFM images showed high surface roughness when ETSC modified SPCE was exposed with maleic anhydride and thus the r_a can be expected to be small as the molecules were very packed.

For ETSC modified SPCE exposed with isoeugenol, the estimated r_a and 2 r_b were 4.73 μm and 21.96 μm, respectively. The estimated r_a and 2 r_b for ETSC modified SPCE exposed with glycerol were 7.08 μm and 40.20 μm, respectively. The increase in the value of r_a and 2 r_b can be explained by the decrease in the average surface of roughness as indicated by the AFM images for ETSC modified SPCE with glycerol and isoeugenol. The ETSC modified SPCE with glycerol recorded the highest r_a and 2 r_b which corresponded to the lowest surface roughness as shown in the AFM image. These trends were also in general agreement with the research work of Casati et al [45].

3.5. Adsorption isotherm studies for ETSC modified SPCE with skin sensitizer

Adsorption studies were performed to probe the binding affinity between cysteine and the skin sensitizers on the ETSC modified SPCE. To understand the binding of the skin sensitizers on the cysteine modified SPCE surface, a graph of C_i/θ_{SC} against C_i was plotted. The plot of C_i/θ_{SC} against C_i yielded a straight line with a coefficient of determination value (R^2) nearly equal to 1 indicating that the experimental data fitted the Langmuir isotherm (Fig. 7).

The slope ranges of these lines were approximately one which suggested strong monolayer adsorption between the skin sensitizer and cysteine surface on ETSC modified SPCE [37,38,45]. This may be because cysteine is a very reactive peptide that has a high affinity towards maleic anhydrides, isoeugenol and glycerol [20].

Binding rate constants were calculated from the intercepts of the plots. Maleic anhydride has a higher and fast binding rate ($5.00 \times 10^{+3}$ M^{-1}) accompanied by a slow dissociation rate of 0.0002 M (Table 4). Isoeugenol and glycerol have a binding rate of $2.00 \times 10^{+03}$ M^{-1} and $1.67 \times 10^{+02}$ M^{-1}, respectively; followed by a fast dissociation rate of 0.0005 M and 0.0059 M, respectively (Fig. 7). The standard binding free energy (ΔG°), measured under the conditions of 1 atm pressure and a temperature of 298 K, is related to the binding constant rate, K_b by the Gibbs relationship where $\Delta G^\circ = -RT\ln K_b$ [36]. For each of the ETSC modified SPCE with maleic anhydride, isoeugenol, and glycerol, the ΔG° was calculated to be $-2.14 \times 10^{+04}$ kJ/mol, $-1.88 \times 10^{+04}$ kJ/mol, and $-1.29 \times 10^{+04}$ kJ/mol, respectively. A negative value of ΔG° indicated spontaneous adsorption of skin sensitizers on ETSC modified SPCE. Similar findings were observed by Migahed et al [37] and Wang et al. [38]. The binding rate represented the adsorption ability of skin sensitizers (maleic anhydrides, isoeugenol and glycerol) on cysteine surface, with the adsorption ability of maleic anhydrides being stronger than isoeugenol and glycerol.

4. Conclusions

ETSC modified SPCE were characterised using FTIR-ATR, AFM and EIS in order to analyse the haptenation of maleic anhydride (extreme/strong skin sensitizer), isoeugenol (moderate skin sensitizer) and glycerol (weak/non skin sensitizer) with cysteine. Extreme/strong skin sensitizer recorded high $\Delta R_{CT}^{skinsensitizer}$ value compared to moderate and weak/non skin sensitizer. FTIR–ATR data analysis suggested the presence of maleic anhydride, isoeugenol, and glycerol after the skin sensitizers interacted with the ETSC modified SPCE. Also, the presence of a stretch of C—S bond suggested the immobilisation of cysteine on the ETSC modified SPCE's surface. AFM image of ETSC modified SPCE exposed with maleic anhydride showed a very high surface roughness (R_a = 35.59 nm). The R_a of ETSC modified SPCE modified SPCE (from AFM image) exposed with isoeugenol and glycerol were 16.74 nm and 10.62 nm, respectively. The ETSC modified SPCE exposed with maleic anhydride reported the highest estimation of θ^{IS} of 0.98 with r_a and $2r_b$ of 2.50 μm and 15.99 μm, respectively. While the θ^{IS} for ETSC modified SPCE exposed with isoeugenol and glycerol were 0.9536 and 0.8757, respectively. The kinetic studies of the adsorption of skin sensitizers on ETSC modified SPCE showed that the adsorption of skin sensitizers followed Langmuir isotherm. The binding affinity of maleic anhydride was highest ($5.00 \times 10^{+03}$ M^{-1}) followed by isoeugenol ($2.00 \times 10^{+03}$ M^{-1}) and glycerol ($1.67 \times 10^{+02}$ M^{-1}). The results of this study suggest that ETSC modified SPCE has the potential to be used for screening of skin sensitizers during early cosmetics and personal care products development.

Funding

This work was supported by the Universiti Teknologi Malaysia (Vot: Q.J130000.2546.14H71); and Ministry of Higher Education (MyBrain scholarship).

Declaration of Competing Interest

The authors declare that they have no known competing financial interests or personal relationships that could have appeared to influence the work reported in this paper.

References

[1] K. Saito, O. Takenouchi, Y. Nukada, M. Miyazawa, H. Sakaguchi, An *in vitro* skin sensitization assay termed EpiSens A for broad sets of chemicals including lipophilic chemicals and pre/pro–haptens, Toxicol. In Vitro 40 (2017) 11–25.

[2] L. Kostner, F. Anzengruber, C. Guillod, M. Recher, P. Schmid-Grendelmeier, A.A. Navarini, Allergic contact dermatitis, Immunol. Allergy Clin. North Am. 37 (1) (2017) 141–152.

[3] I. Chipinda, M. Justin Hettick, D. Paul Siegel, Haptenation: chemical reactivity and protein binding, J. Allergy Clin. Immunol. (2011) 1–11.

[4] G.F. Gerberick, C.A. Ryan, P.S. Kern, R.J. Dearman, I. Kimber, G.Y. Patlewicz, D.A. Basketter, A chemical dataset for evaluation of alternative approaches to skin–sensitization testing, Contact Derm. 50 (5) (2004) 274–288.

[5] A.O. Aptula, G. Patlewicz, D.W. Roberts, Skin sensitization: reaction mechanistic applicability domains for structure–activity relationships, Chem. Res. Toxicol. 1420–1426 (2005).

[6] R. Soleri, H. Demey, S.A. Tria, A. Guiseppi-Elie, A. Hassine, C. Gonzalez, I. Bazin, Peptide conjugated chitosan foam as a novel approach for capture–purification and rapid detection of hapten –Example of ochratoxin A, Biosens. Bioelectron. 67 (2015) 634–641.

[7] P. Botham, D. Basketter, T. Maurer, D. Mueller, M. Potokar, W.J. Bontinck, Skin sensitization–a critical review of predictive test methods in animals and man, Food Chem. Toxicol. 29 (1991) 275–286.

[8] V. Zuang, A. Dura, D. Asturiol Bofill, S. Batista Leite, E. Berggren, C. Bernasconi, S. Bopp, G. Bowe, I. Campia, D. Carpi, S. Casati, S. Coecke, T. Cole, R. Corvi, P. Deceuninck, S. Fortaner Torrent, A. Franco, L. Gribaldo, E. Grignard, M. Halder, M. Holloway, A. Kienzler, P. Macko, F. Madia, A. Milcamps, S. Morath, S. Munn, A, Paini, T. Palosaari, F. Pistollato, A. Price, M. Prieto Peraita, J. Sund, J. Viegas Barroso, C. Wittwehr, A. Worth, M. Whelan, EURL ECVAM Status Report on the Development, Validation and Regulatory Acceptance of Alternative Methods and Approaches (2019).

[9] A. Angers-Loustau, L. Tosti, S. Casati, The regulatory use of the local lymph node assay for the notification of new chemicals in Europe, Regul. Toxicol. Pharmacol. 60 (2011) 300–307.

[10] G.F. Gerberick, Development of a Peptide reactivity assay for screening contact allergens, Toxicol. Sci. 81 (2) (2004) 332–343.

[11] M. Fujita, Y. Yamamoto, H. Tahara, T. Kasahara, Y. Jimbo, T. Hioki, Development of a prediction method for skin sensitization using novel cysteine and lysine derivatives, J. Pharmacol. Toxicol. Methods 70 (1) (2014) 94–105.

[12] Y. Yamamoto, H. Tahara, R. Usami, T. Kasahara, Y. Jimbo, T. Hioki, M. Fujita, A novel *in chemico* method to detect skin sensitizers in highly diluted reaction conditions, J. Appl. Toxicol. 35 (11) (2015) 1348–1360.

[13] M. Fujita, Y. Yamamoto, S. Watanabe, T. Sugawara, K. Wakabayashi, Y. Tahara, N. Horie, K. Fujimoto, K. Kusakari, Y. Kurokawa, T. Kawakami, K. Kojima, H. Kojima, A. Ono, Y. Katsuoka, H. Tanabe, H. Yokoyama, T. Kasahara, Cause of and counter measures for the oxidation of the cysteine–derived reagent used in the amino acid derivative reactivity assay, J. Appl. Toxicol. 1–18 (2018).

[14] OECD 2019, Draft validation report: amino acid derivative reactivity assay (ADRA) – JaCVAM Validation Study Report. Series on testing and Assessment n° 304. Organisation for Economic Cooperation and Development, Paris.

[15] EC EURL ECVAM 2012, Direct peptide reactivity assay (DPRA) validation study report 74. http://ihcp.jrc.ec.europa.eu/our_labs/eurl–ecvam/eurl–ecvam–recommendations/eurl–ecvamrecommendation–on–the–direct–peptide–reactivity–assay–dpra

[16] A. Natsch, C.A. Ryan, L. Foertsch, R. Emter, J. Jaworska, F. Gerberick, P. Kern, A dataset on 145 chemicals tested in alternative assays for skin sensitization undergoing prevalidation, J. Appl. Toxicol. 1–16 (2013).

[17] A.G. Chittiboyina, C. Avonto, D. Rua, I.A. Khan, Alternative testing methods for skin sensitization: NMR spectroscopy for probing the reactivity and classification of potential skin sensitizers, Chem. Res. Toxicol. 28 (9) (2015) 1704–1714.

[18] E. Andres, A. Obry, A. Hundt, C. Dini, Successful evaluation of sensitization by DPRA assay coupled with Mass Spectrometry detection, Toxicol. Lett. 258 (2016) S146.

[19] Z. Wei, Y. Fang, M.L. Gosztyla, A.J. Li, W. Huang, C.A. LeClair, A. Simeonov, D. Tao, M. Xia, A direct peptide reactivity assay using a high–throughput mass spectrometry screening platform for detection of skin sensitizer, Toxicol. Lett. 338 (2021) 67–77.

[20] C. Achilleos, M. Tailhardat, P. Courtellemont, B.L. Varlet, D. Dupont, Investigation of surface plasmon resonance biosensor for skin sensitizers studies, Toxicol. Vitro 23 (2) (2009) 308–318.

[21] S.C.B. Gopinath, Biosensing Applications of surface plasmon resonance–based Biacore technology, Sens. Actuators B Chem. 150 (2) (2010) 722–733.

[22] Q. Liu, C. Wu, H. Cai, N. Hu, J. Zhou, P. Wang, Cell–based biosensors and their application in biomedicine, Chem. Rev. 114 (2014) 6423–6461.

[23] H. Nguyen, J. Park, S. Kang, M. Kim, Surface plasmon resonance: a versatile technique for biosensor applications, Sensors 15 (5) (2015) 10481–10510.

[24] T.U. Noh, A. Abd Aziz, Estimation of the surface area of a screen–printed carbon electrode modified with gold nanoparticles and cysteine using electrochemical impedance spectroscopy, Chem. Eng. Trans. 63 (2018) 529–534.

[25] R. Radhakrishnan, I.I. Suni, C.S. Bever, B.D. Hammock, Impedance biosensors: Applications to sustainability and remaining technical challenges, ACS Sustain. Chem. Eng. 2 (7) (2014) 1649–1655.

[26] P. Jiang, Y. Wang, L. Zhao, C. Ji, D. Chen, L. Nie, Applications of Gold Nanoparticles in Non-Optical Biosensors, Nanomaterials 8 (12) (2018) 977.

[27] Y. Zhao, Y. Hu, J. Hou, Z. Jia, D. Zhong, S. Zhou, D. Huo, M. Yang, C. Hou, Electrochemical biointerface based on electrodeposition AuNPs on 3D graphene aerogel: direct electron transfer of Cytochrome c and hydrogen peroxide sensing, J. Electroanal. Chem. 842 (2019) 16–23.

[28] A. Mocanua, C. Ileana, T. Gheorghe, B. Liviu-Dorel, H. Ossi, T.-c. Maria, Self–assembly characteristics of AuNPs in the presence of cysteine, Colloids Surf. A Physicochem Eng Asp. 338 (1–3) (2009) 93–101.

[29] A. Dolati, I. Imanieh, The effect of cysteine on electrodeposition of AuNPs, Mater. Sci. Eng. B. 176 (16) (2011) 1307–1312.

[30] A.A.P. Ferreira, C.S. Fugivara, S. Barrozo, P.H. Suegama, H. Yamanaka, A.V. Benedetti, Electrochemical and spectroscopic characterization of screen–printed gold–based electrodes modified with self–assembled monolayers and Tc85 protein, J. Electroanal. Chem. 634 (2009) 111–122.

[31] J.S. Daniels, N. Pourmand, Label free impedance biosensor: opportunities and challenges, Electroanal. 19 (12) (2008) 239–1257.

[32] B. Wang, R. Jing, H. Qi, Q. Gao, C. Zhang, Label–free electrochemical impedance peptide–based biosensor for the detection of cardiac troponin I incorporating gold nanoparticles modified carbon electrode, J. Electroanal. Chem. 781 (2016) 212–217.

[33] H.-B. Wang, H.-D. Zhang, S.-P. Xu, T. Gan, K.-J. Huang, Y.-M. Liu, A sensitive and label–free electrochemical impedance biosensor for protein detection based on terminal protection of small molecule–linked DNA, Sens. and Actuators B: Chem. 194 (2014) 478–483.

[34] H. Matsuda, K. Tokuda, T. Gueshi, Voltammetry at partially covered electrodes: Part III. Faradaic impedance measurements at model electrodes, J. Electroanal. Chem. 102 (1979) 41–48.

[35] H.O. Finklea, D.A. Sinder, J. Fedyk, E. Sabatini, Y. Gaini, I. Rubinstein, Characterization of octadecanethiol–coated gold electrodes as microarray electrodes by cyclic voltammetry and AC impedance spectroscopy, Langmuir 9 (1993) 3660.

[36] D. Xing, L. Yi, X. Yuan-Ling, A. Shi-Meng, L. Jing, S. Peng, J. Xing-Lai, L. Shu-Qun, Insights into protein–ligand interactions: mechanisms, models, and methods, Int. J. Mol. Sci 17 (2) (2016) 144–178.

[37] M. Migahed, E.M.S. Azzam, S.M.I. Morsy, Electrochemical behaviour of carbon steel in acid chloride solution in the presence of dodecyl cysteine hydrochloride self–assembled on gold nanoparticles, Corros. Sci. 51 (2009) 1636–1644.

[38] C. Wang, C. Zou, Y. Cao, Electrochemical and isothermal adsorption studies on corrosion inhibition performance of β–cyclodextrin grafted polyacrylamide for X80 steel in oil and gas production, J. Mol. Struc. 1228 (2021) 129737.

[39] J. Coates, Interpretation of infrared spectra, A practical approach interpretation of infrared spectra, A practical approach, Encycl. Anal. Chem. (2000) 10815–10837.

[40] I. Feliciano-Ramos, M. Caban-Acevedo, M. Aulice Scibioh, C.R. Cabrera, Self–assembled monolayers of L–cysteine on palladium electrodes, J. Electroanal. Chem. 650 (1) (2010) 98–104.

[41] S. Mukdasai, V. Langsi, M. Pravda, S. Srijaranai, J.D. Glennon, A highly sensitive electrochemical determination of norepinephrine using l–cysteine self–assembled monolayers over gold nanoparticles/multi–walled carbon nanotubes electrode in the presence of sodium dodecyl sulfate, Sens. and Actuators B: Chem. 236 (2016) 126–135.

[42] D. Basketter, S. Casati, G. Gerberick, G. Frank, G. Peter, P. Barry, W. Andrew, Skin sensitisation, Altern Lab Anim. 33 (2005) 83–103.

[43] M. Divkovic, C.K. Pease, G.F. Gerberick, D. Basketter, Hapten–protein binding: From theory to practical application in the *in vitro* prediction of skin sensitization, Contact Derm. 53 (2005) 189–200.

[44] H. Ivanova, G. Dimitrova, C. Kuseva, T. W. Schultz, O. G. Mekenyan, Modeling hazard assessment of chemicals based on adducts formation. I. A basis for inclusion of kinetic factors in simulating skin sensitization, Comput. Toxicol., 100130.

[45] S. Casati, K. Aschberger, D. Basketter, S. Dimitrov, C. Dumont, A. Karlberg, P. Lepoittevin, G. Patlewicz, W. David, A. Worth, Ability of non–animal methods for skin sensitisation to detect pre– and pro–haptens, in: Report and Recommendations of an EURL ECVAM Expert Meeting, 2016, pp. 4–19.